Clays and Clay Minerals, Vol. 40, No. 2, 145–150, 1992.

COMPOSITION AND PROPERTIES OF SYNTHETIC HYDROTALCITES

C. MISRA AND A. J. PERROTTA

Alcoa Laboratories, Alcoa Center, Pennsylvania 15069

Abstract—Hydrotalcites of high aluminum content have been synthesized from aluminate liquors of varying composition and activated magnesia obtained by calcination of hydroxide or hydroxycarbonate precursors. Lattice parameter measurements and chemical analyses of 21 synthetic hydrotalcites show that the aluminum substitution $\left(X = \frac{Al}{Al + Mg}\right)$ for most of the products is about 0.35, which is at the maximum experimentally-observed limit of solid solubility. Pillared hydrotalcites were also prepared by molybdate, chromate, and silicate anion replacement. A maximum distance of 10.4 Å between the brucite-like layers was observed for the $Mo_7O_{24}^{6-}$ intercalated material.

Key Words—Aluminate liquor, Aluminum substitution, Anion replacement, Hydrotalcite, Magnesium oxide, Pillaring.

INTRODUCTION

A process that is capable of producing hydrotalcite with high aluminum substitution utilizes the reaction of MgO with carbonate containing sodium aluminate solution. The MgO/Al_2O_3 ratio can be as low as 3.3 compared to the value of 6.0 for "normal" hydrotalcite and 4.5 for other commercially available hydrotalcite (source, Kyowa Chemicals, 1988). The purpose of this study is to discuss the synthesis, composition, and property of hydrotalcites formed by this process.

Synthetic hydrotalcite has a structure consisting of brucite-like octahedral layers with compositions of the type $[R_{1-x}^{2+}R_x^{3+}(OH)_2]^{+x}R_{x/n}^{-n}\cdot yH_2O$. The net positive charge of the brucite-like octahedral layers is balanced by an equal negative charge from the interlayer anions. Water molecules occupy residual space with the compensating anions in the interlayer region. The early work on the composition and structures of hydrotalcite was reviewed by Frondel (1941). Structural studies have been done by Allman and Lohse (1966), Ingram and Taylor (1967), Allman and Jepsen (1969), Taylor (1969), and Brown and Gastuche (1967).

Numerous synthesis studies have been done on hydrotalcite (Mascolo and Marino, 1980; Taylor, 1984; Miyata, 1980; Pausch *et al.*, 1986; Gastuche *et al.*, 1967). Aluminum contents of both natural and synthetic hydrotalcite-like phases show an approximately linear relationship to a_0 of the brucite-like layer. Additional studies on the intercalation of various inorganic or organic anions either by direct synthesis or ion exchange and their effect of c_0 have also been done (Brindley and Kikkawa, 1979, 1980; Miyata, 1983; Giannelis *et al.*, 1987; Drezdzon, 1988; Chibwe and Jones, 1989; Dimotakis and Pinnavaia, 1990).

EXPERIMENTAL

Activated magnesia was prepared by calcination of technical grade magnesium hydroxide $[Mg(OH)_2]$ and magnesium hydroxy carbonate $[Mg_5(CO_3)_4(OH)_2\cdot 4H_2O]$. Aluminate liquors of different compositions were prepared by dissolving aluminum hydroxide (Alcoa C-30) in NaOH solution at 150°C. Sodium carbonate was added for TC/TA control, where TC is sodium hydroxide caustic expressed as sodium carbonate and TA is the sum of total alkali, which includes both the sodium hydroxide and sodium carbonate. Syntheses were carried out in sealed high-density polyethylene bottles rotating end-over-end in a water bath maintained at 90°–91°C. Run time was 4 hr using 10 g of equivalent magnesia and 250 ml of liquor in each case. At the end of the run, the product was filtered, washed with distilled water, and dried overnight at 105°C.

Hydrotalcite products were analyzed by X-ray diffraction (XRD); chemical analysis by atomic absorption for Mg, Al, and Na; scanning and transmission electron microscopy of selected samples; and product weight and weight loss to 220°C and 1200°C. In addition, the starting and final liquors were analyzed for Al_2O_3, TC, Na_2CO_3, and TA using an automatic titrator. The lattice parameter a_0 was determined at scanning speeds of $\frac{1}{4}°2\theta$ per minute of the (110) reflection utilizing an internal correction standard of alpha alumina in each run.

Anion replacement to give pillared hydrotalcites was carried out by a calcination-reformation method (described below). An experimental hydrotalcite, sample 21, was activated at 500°C for 4 hr. The calcined product was stored in air-tight bottles. Anion replacement was carried out by agitating 300 g of calcined material with 2500 ml of 1 N solution $[(NH_4)_6Mo_7O_{24}\cdot 4H_2O$, $Na_2Cr_2O_7\cdot 2H_2O$, $Na_2SiO_3\cdot 9H_2O]$ of the salt of the anion. Agitation was continued over 24 hr in a N_2 atmosphere at room temperature. In some cases, a temperature of 40°–45°C was maintained to insure complete solubility of the salt. A 5 liter stainless steel reaction vessel equipped with an anchor-type agitator was em-

Copyright © 1992, The Clay Minerals Society

https://doi.org/10.1346/CCMN.1992.0400202 Published online by Cambridge University Press

Table 1. MgO preparation and sources.

No.	Material no.	Source	Calcination temp. (°C)[1]	Weight loss (%)	BET surface area m^2/g	XRD identity
1	$Mg(OH)_2$-0	$Mg(OH)_2$	—	—	35	$Mg(OH)_2$
2	$Mg(OH)_2$-300	$Mg(OH)_2$	300	5.4	46	$Mg(OH)_2$ + minor MgO
3	$Mg(OH)_2$-400	$Mg(OH)_2$	400	29.9	97	Virtually all MgO
4	$Mg(OH)_2$-500	$Mg(OH)_2$	500	29.8	52	Entirely MgO
5	$Mg(OH)_2$-550	$Mg(OH)_2$	550	30.0	47	Entirely MgO
6	$Mg(OH)_2$-600	$Mg(OH)_2$	600	30.3	42	Entirely MgO
7	$MgCO_3$-0	$Mg_5(CO_3)_4(OH)_2 \cdot 4H_2O$	—	—	21	$Mg_5(CO_3)_4(OH)_2 \cdot 4H_2O$
8	$MgCO_3$-300	$Mg_5(CO_3)_4(OH)_2 \cdot 4H_2O$	300	20.7	39	Transition form
9	$MgCO_3$-400	$Mg_5(CO_3)_4(OH)_2 \cdot 4H_2O$	400	52.3	255	Entirely MgO
10	$MgCO_3$-500	$Mg_5(CO_3)_4(OH)_2 \cdot 4H_2O$	500	54.6	172	Entirely MgO
11	$MgCO_3$-600	$Mg_5(CO_3)_4(OH)_2 \cdot 4H_2O$	600	55.3	99	Entirely MgO
12	$MgCO_3$-700	$Mg_5(CO_3)_4(OH)_2 \cdot 4H_2O$	700	56.0	75	Entirely MgO
13	$MgCO_3$-800	$Mg_5(CO_3)_4(OH)_2 \cdot 4H_2O$	800	56.3	56	Entirely MgO
14	AHTC-A	Hydrotalcite	500	38.0	ND	Amorphous
15	AHTC-B	Hydrotalcite	500	39.6	ND	Amorphous
16	AHTC-C	Hydrotalcite	500	39.1	ND	Amorphous
17	AHTC-D	Hydrotalcite	500	39.1	ND	Amorphous + MgO

[1] Calcined for 4 hr.

ployed for all the runs. Material was removed at the end of the reaction period, filtered, displacement-washed with hot distilled water, and dried at 105°C. Samples were analyzed for chemical composition, XRD identification, and thermal (TGA, DSC) behavior.

RESULTS AND DISCUSSION

The data on activated magnesia used in the preparation of hydrotalcite is given in Table 1. The brucite precursor shows a transition to MgO between 300°C to 400°C at a calcination time of 4 hr. The maximum surface area of nearly 100 m^2/g occurs at 400°C where virtually all of the brucite has been converted to magnesia. Similar calcination experiments on magnesium hydroxy carbonate show complete transition to magnesia at 400°C with a surface area of about 250 m^2/g, indicating the potential for a reactive precursor for hydrotalcite formation. For both the brucite and magnesium hydroxy carbonate, the weight loss remained essentially constant above 400°C to the highest calcination temperatures, corroborating the transition to magnesia as seen by X-ray analysis.

Table 2. Analysis of aluminate liquors used for synthesis.

No.	Description	TA g/liter	TC g/liter	Al_2O_3 g/liter	R	Na_2CO_3 g/liter	TC/TA
Oliq - 1	Starting liquor	202.1	158.0	87.8	0.556	44.1	0.782
Oliq - 2	Starting liquor	194.9	153.5	64.9	0.423	41.4	0.788
Oliq - 3	Starting liquor	254.4	244.5	135.8	0.555	9.9	0.961
Oliq - 4	Starting liquor	204.9	164.3	78.6	0.478	40.6	0.802
Fliq - 1	Final liquor, run 1	212.1	183.6	68.2	0.371	28.6	0.865
Fliq - 2	Final liquor, run 2	212.6	182.7	67.5	0.369	29.9	0.859
Fliq - 3	Final liquor, run 3	213.4	185.1	66.8	0.361	28.3	0.867
Fliq - 4	Final liquor, run 4	210.6	182.0	71.6	0.393	28.6	0.864
Fliq - 5	Final liquor, run 5	211.6	184.6	69.6	0.377	27.0	0.872
Fliq - 6	Final liquor, run 6	213.4	185.4	69.7	0.376	28.0	0.869
Fliq - 7	Final liquor, run 7	212.2	185.8	68.2	0.367	26.4	0.875
Fliq - 8	Final liquor, run 8	212.2	185.5	67.4	0.363	26.7	0.874
Fliq - 9	Final liquor, run 9	203.7	177.5	44.6	0.251	26.2	0.871
Fliq - 10	Final liquor, run 10	204.9	176.8	44.4	0.251	28.0	0.863
Fliq - 11	Final liquor, run 11	207.3	175.0	44.6	0.255	32.3	0.844
Fliq - 12	Final liquor, run 12	217.8	181.5	53.2	0.293	36.3	0.833
Fliq - 13	Final liquor, run 13	152.5	128.2	37.9	0.295	24.3	0.841
Fliq - 14	Final liquor, run 14	191.9	164.7	46.0	0.279	27.2	0.858
Fliq - 15	Final liquor, run 15	204.3	177.1	46.1	0.260	27.2	0.867
Fliq - 16	Final liquor, run 16	205.4	178.7	44.9	0.251	26.7	0.870
Fliq - 17	Final liquor, run 17	266.5	262.2	117.6	0.449	4.3	0.984
Fliq - 18	Final liquor, run 18	208.5	176.4	80.0	0.454	32.1	0.846
Fliq - 19	Final liquor, run 19	212.6	179.2	79.7	0.445	33.4	0.843
Fliq - 20	Final liquor, run 20	191.1	160.4	71.5	0.445	30.7	0.839
Fliq - 21	Final liquor, run 21	211.7	177.2	76.6	0.432	34.5	0.837

https://doi.org/10.1346/CCMN.1992.0400202 Published online by Cambridge University Press

Table 3. Synthesis experiments.

Run no.	MgO used	Start liquor	Product weight, g	Product nature	Weight loss 220°C	L.O.I. 1200°C
1	$Mg(OH)_2$-400	Oliq - 1	26.228	Lumpy	16.192	43.85
2	$Mg(OH)_2$-500	Oliq - 1	26.380	Powder	16.219	43.81
3	$Mg(OH)_2$-600	Oliq - 1	26.346	Powder	16.250	43.52
4	$MgCO_3$-400	Oliq - 1	24.440	Lumpy	16.468	44.40
5	$MgCO_3$-500	Oliq - 1	25.810	Lumpy	16.045	44.65
6	$MgCO_3$-600	Oliq - 1	26.326	Lumpy	15.592	44.21
7	$MgCO_3$-700	Oliq - 1	26.609	Powder	15.803	44.06
8	$MgCO_3$-800	Oliq - 1	26.852	Powder	15.582	44.17
9	$Mg(OH)_2$-400	Oliq - 2	25.864	Powder	15.274	43.19
10	$Mg(OH)_2$-500	Oliq - 2	26.057	Powder	15.314	43.08
11	$Mg(OH)_2$-600	Oliq - 2	26.212	Powder	15.314	43.08
12	$MgCO_3$-400	Oliq - 2	23.078	Lumpy	14.851	44.04
13	$MgCO_3$-500	Oliq - 2	23.630	Lumpy	14.306	43.65
14	$MgCO_3$-600	Oliq - 2	24.842	Lumpy	14.222	43.68
15	$MgCO_3$-700	Oliq - 2	26.038	Powder	14.511	43.64
16	$MgCO_3$-800	Oliq - 2	26.517	Powder	14.516	43.56
17	$Mg(OH)_2$-550	Oliq - 3	25.709	Powder	17.558	40.88
18	AHTC-A[1]	Oliq - 4	15.567	Powder	15.596	42.80
19	AHTC-B[1]	Oliq - 4	16.504	Powder	14.849	43.15
20	AHTC-C[1]	Oliq - 4	16.179	Powder	14.784	32.14
21	AHTC-D[2]	Oliq - 4	16.426	Powder	13.221	40.17

[1] AHTC-A, B, C are reactivated hydrotalcites from runs 3, 4, and 5, respectively.
[2] Activated product from Arkansas (Sample P-2996).

The analysis of the aluminate liquors (Table 2) shows alumina concentrations ranging from 64.9 to 135.8 g/liter. The results of the hydrotalcite syntheses using these four liquors and the two magnesia sources are given in Table 3. Recrystallization experiments (runs 18–21) were also done using calcined hydrotalcites from earlier experiments. In addition, a hydrotalcite from the Alcoa plant (Bauxite, Arkansas) was used as a comparative base showing a slightly smaller weight loss to 200°C. Typically, the loss on ignition to 1200°C giving anhydrous products lies between 40–45% weight loss.

The product analyses (Table 4) give a range of magnesia-to-alumina ratios ranging from 3.26 to 4.84. These molar ratios are all lower than the value of six given for the mineral hydrotalcite, $Mg_6Al_2(OH)_{16}CO_3 \cdot 4H_2O$. The interlayer water, determined by weight loss to 220°C, ranges from 3.39 to 4.29 moles per mole of hydrotalcite, which is in reasonable agreement to that given for hydrotalcite.

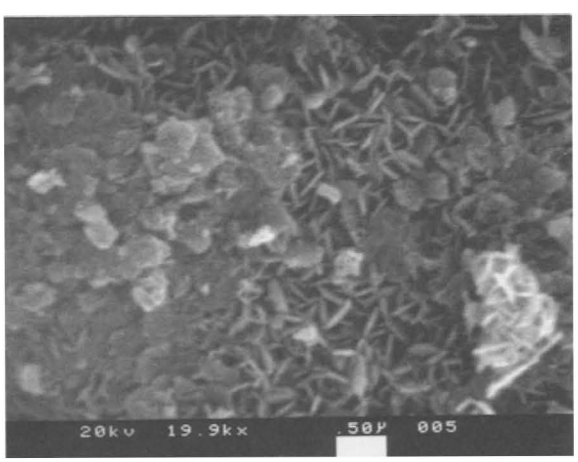


Figure 1. Scanning electron micrograph of original hydrotalcite (run 2).

Table 4. Product analyses.

Run no.	% Mg	% Al	% Na	Molar MgO/Al_2O_3	Molar[1] H_2O/product
1	20.5	12.9	0.01	3.53	3.766
2	20.4	12.9	0.01	3.51	3.772
3	20.5	12.6	0.01	3.61	3.869
4	20.8	11.7	0.04	3.95	4.223
5	20.4	11.7	0.14	3.87	4.114
6	20.6	12.3	0.16	3.72	3.803
7	19.8	12.3	0.15	3.58	3.854
8	20.3	12.4	0.02	3.64	3.770
9	20.4	12.3	0.02	3.68	3.725
10	20.6	12.3	0.01	3.72	3.735
11	20.8	12.2	0.01	3.78	3.766
12	22.3	10.7	0.02	4.63	4.164
13	21.8	10.0	0.01	4.84	4.292
14	22.2	10.6	0.03	4.65	4.025
15	21.1	11.5	0.02	4.07	3.785
16	18.8	12.2	0.03	3.42	3.570
17	20.7	13.1	<0.01	3.51	4.021
18	19.6	12.9	0.02	3.37	3.627
19	19.1	13.0	0.03	3.26	3.427
20	19.6	12.9	0.02	3.37	3.438
21	22.1	11.7	0.02	4.20	3.390
22+	21.1	9.7	ND	4.83	ND

[1] Interlayer water was calculated from weight loss to 220°C.
21 Arkansas hydrotalcite, activated and reacted Oliq - 4 as on Table 3.
22+ Original hydrotalcite from Arkansas (Sample P-2996).

https://doi.org/10.1346/CCMN.1992.0400202 Published online by Cambridge University Press

Table 5. Aluminum content and cell parameter (a_0).

Sample	$\frac{Al}{Mg + Al}$	a (±0.001 Å)
1	0.36	3.039
2	0.36	3.039
3	0.357	3.040
4	0.336	3.044
5	0.34	3.044
6	0.35	3.041
7	0.36	3.042
8	0.355	3.040
9	0.352	3.040
10	0.35	3.040
11	0.346	3.040
12	0.30	3.049
13	0.29	3.050
14	0.30	3.046
15	0.33	3.043
16	0.369	3.042
17	0.363	3.040
18	0.372	3.038
19	0.380	3.039
20	0.372	3.039
21[3]	0.323 free MgO present	3.038
22[1]	0.308 (Kyowa) 0.323 (ours)	3.043
23[2]	0.25	3.06

[1] Kyowa hydrotalcite.
[2] Neumann and Bergstol; Mineralogical Museum, Olso, Norway (see card 14.191, JCPDS).
[3] Arkansas sample reprocessed with Oliq - 4 in Table 3 used in pillaring experiments.

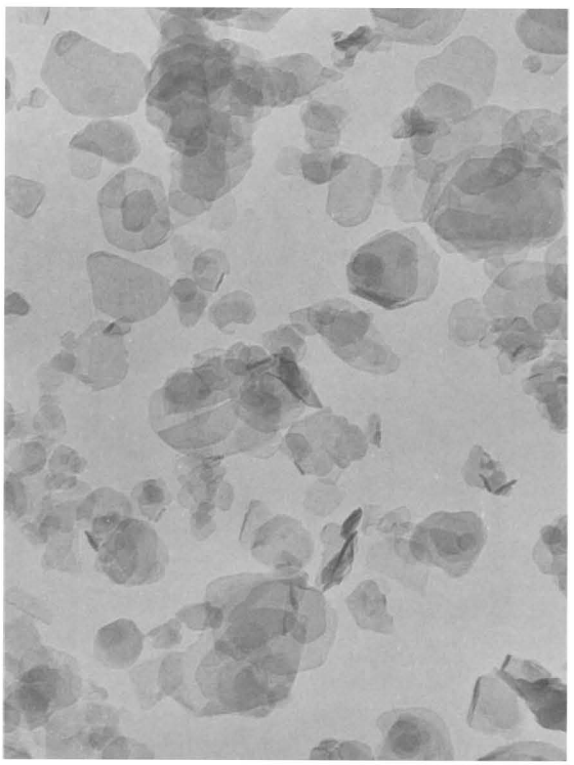


Figure 2. Transmission electron micrograph of original hydrotalcite (run 2, 62,000×).

XRD analysis showed the products to be pure hydrotalcite except for the product from Arkansas plant (run 21) that contained unreacted MgO.

The appearance of a typical product (run 2) is shown in the SEM picture (Figure 1). It consists of agglomerates of thin, hexagonal, plate-like crystals of 0.2–0.5 μm in size. This is further displayed in the higher magnification TEM picture (Figure 2) of the deagglomerated product.

The changes in a_0 that are most sensitive to aluminum substitution in the brucite-like layer as a function of aluminum content determined in the final phase are given in Table 5. These are also plotted in Figure 3 at a similar scale to that given by Pausch *et al.* (1986). This allows comparison of our results to the curve generated previously using the a_0 of natural and synthetic hydrotalcite-like phases as a function of Al-contents from five different studies. Approximately one-third of our synthetic hydrotalcites have a higher aluminum content ($X > 0.32$) given by the "knee" in the curve of Pausch *et al.* (1986), and have an appropriate lattice parameter, a_0, correspondingly lower than

Table 6. Pillaring anion substitution, composition, and cell expansion.

Name	Pillaring[2] anion (X)	Chemical composition % Mg	% Al	% (X)	Distance between brucite layers Å	After activation at 500°C for 4 hr: Surface area m^2/g	Pore diameter Å
1. Normal hydrotalcite[1] ($Mg_6Al_2(OH)_{16}CO_3 \cdot 4H_2O$)	None (CO_3^{2-} is the usual anion present)	21.5	10.0	—	7.69	—	—
2. Precursor hydrotalcite (sample 21)	None (CO_3^{2-} is the usual anion present)	22.1	11.7	—	7.695	162	73
3. Pillared hydrotalcite "A"	$Cr_2O_7^{2-}$	17.9	12.1	8.1 (Cr)	8.4	18	92
4. Pillared hydrotalcite "B"	$Mo_7O_{24}^{6-}$	13.8	8.2	23.4 (Mo)	9.6–10.4	34	225
5. Pillared hydrotalcite "C"	SiO_3^{2-}	25.1	10.3	6.2 (Si)	7.7	111	56

[1] Neumann and Bergstol; Mineralogical Museum, Oslo, Norway (see card 14.191, JCPDS).
[2] The indicated anions correspond to the anion formula for the starting salt.

https://doi.org/10.1346/CCMN.1992.0400202 Published online by Cambridge University Press

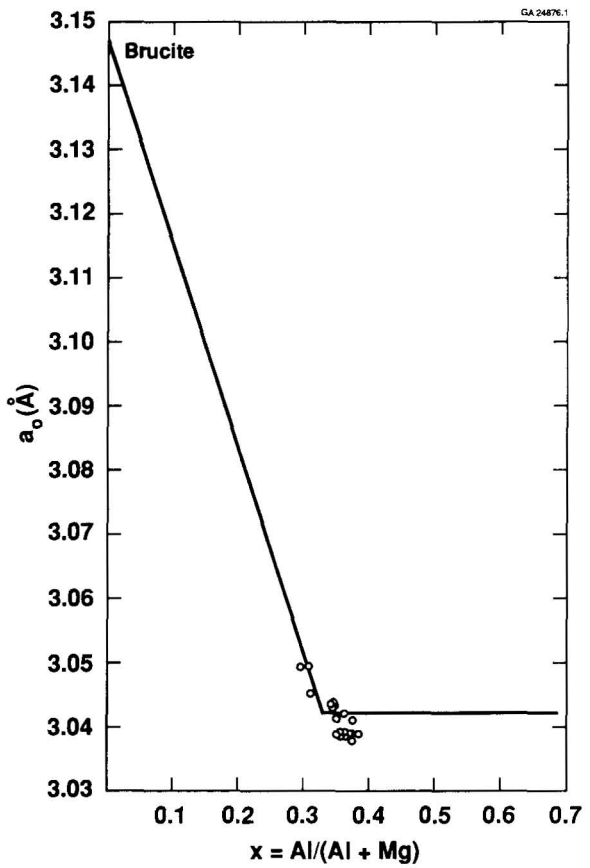


Figure 3. Cell parameters of synthetic hydrotalcite-like phases as a function of aluminum content $X = \frac{Al}{Al + Mg}$. Plotted for comparative analysis at the same scale as given by Pausch *et al.* (1986).

values on the curve. This indicates that our syntheses are capable of producing hydrotalcite-like phases with the maximum amount of aluminum substitution presently possible in the structure. The anion replacement data involving $Cr_2O_7^{2-}$, $Mo_7O_{24}^{6-}$, and SiO_3^{2-} with a hydrotalcite from our Arkansas plant (sample 21) are given in Table 6. The X-ray diffractograms are given in Figure 4. The appearance of the molybdate containing recrystallized hydrotalcite is shown in Figure 5. This product consists of agglomerates of somewhat larger plate-like crystals of 1–2 μm in size.

The distance between the brucite-like layers expanded from 7.69 Å to 8.4 Å when intercalated with $Cr_2O_7^{2-}$ ions. This may be CrO_4^{2-} since equilibrium considerations show that $Cr_2O_7^{2-}$ converts to CrO_4^{2-} under the conditions. The intercalation of $Mo_7O_{24}^{6-}$ ions increased the layer separation to about 9.6 Å, which is less than the 12.2 Å reported by Drezdzon (1988) using terephthalate dianion hydrotalcite for ion exchange. In addition, his chemical analysis showed

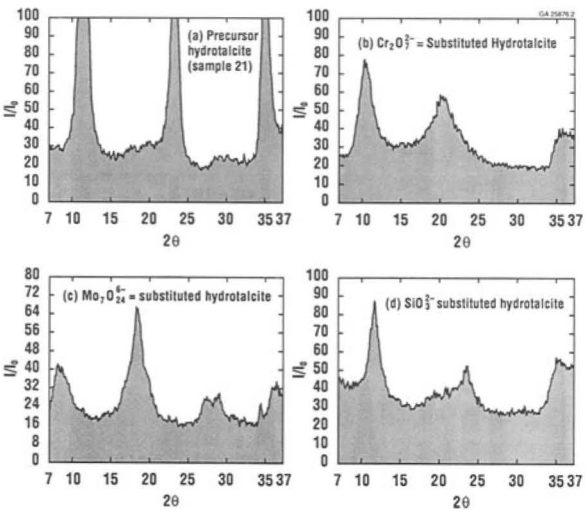


Figure 4. X-ray diffractograms of pillared hydrotalcites. (a) Precursor hydrotalcite (sample 21), (b) $Cr_2O_7^{2-}$-substituted hydrotalcite, (c) $Mo_7O_{24}^{6-}$-substituted hydrotalcite, (d) SiO_3^{2-}-substituted hydrotalcite.

more Mo (28.7%) and correspondingly less Mg (13.25%) and Al (7.2%) than ours, which should lead to a larger layer spacing. It is interesting that for both molybdenum-intercalated species (Drezdzon (1988) and ours), the X-ray intensities observed for the (001) and (002) peaks are reversed relative to the CO_3^{2-} base hydrotalcites. In the case of silication, although 6.2% Si was found chemically, the interlayer spacing is essentially the same as the original hydrotalcite (7.7 Å). In all three intercalated compounds, the (220) reflection was essentially unaffected at about 1.53 Å, as expected.

Chibwe and Jones (1989) exposed calcined hydrotalcite to a $K_2Cr_2O_7$ solution and obtained a layer separation of 5.2 Å by the intercalation of $Cr_2O_7^{2-}$ ions.

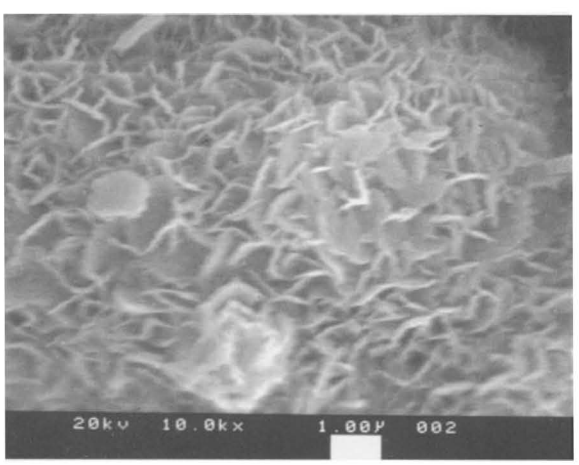


Figure 5. Scanning electron micrograph of ammonium molybdate-pillared hydrotalcite.

https://doi.org/10.1346/CCMN.1992.0400202 Published online by Cambridge University Press

With an approximate thickness of the brucite layer of 4.8 Å, the interlayer height is about 10 Å compared to the 8.4 Å obtained in our work. Dimotakis and Pinnavaia (1990) proposed the use of well-ordered organic anion derivatives as precursors to pillared derivatives and gave an example of the synthesis of hydrotalcite interlayered by the keggin ion species $H_2W_{12}O_{40}^{6-}$ (d = 14.8 Å).

In summary, the syntheses studied in this investigation indicate that a high aluminum content ($X > 0.32$) can be obtained in hydrotalcite using our synthesis method. In addition, these materials can be intercalated with some complex ions using a calcination-reformation method. Further work is needed to establish the identity of the intercalated ion and the resulting crystal structure of the intercalated hydrotalcite.

REFERENCES

Allman, R. and Jepsen, H. P. (1969) Die Struktur des Hydrotalkits: *Neues Jahrb. Mineral. Monatsh.,* 544–551.

Allman, R. and Lohse, H. H. (1966) Die Kristallstruktur des Sjöjrenits und eines Umwandlungsproduktes des Koenenits (= Chlor-Manasseits): *Neues Jahrb. Mineral. Monatsh.,* 161–181.

Brindley, G. W. and Kikkawa, S. (1979) A crystal-chemical study of Mg, Al, and Ni, Al hydroxy-perchlorates and hydroxy-carbonates: *Amer. Mineral.* **64,** 836–843.

Brindley, G. W. and Kikkawa, S. (1980) Thermal behavior of hydrotalcite and of anion-exchanged forms of hydrotalcite: *Clays & Clay Minerals* **28,** 87–91.

Brown, G. and Gastuche, M. C. (1967) Mixed magnesium-aluminum hydroxides. II Structural chemistry of synthetic hydroxy-carbonates and related minerals and compounds: *Clay Miner.* **7,** 193–201.

Chibwe, K. and Jones, W. (1989) Intercalation of organic and inorganic anions into layered double hydroxides: *J. Chem. Soc., Chem. Commun.,* 926–927.

Dimotakis, E. D. and Pinnavaia, T. J. (1990) New route to layered double hydroxides intercalated by organic anions: Precursors to polyoxometalate-pillared derivatives: *Inorg. Chem.* **29,** 2393–2394.

Drezdzon, M. A. (1988) Synthesis of isopolymetalate-pillared hydrotalcite via organic anion-pillared precursors: *Inorg. Chem.* **27,** 4628–4632.

Frondel, C. (1941) Constitution and polymorphism of the pyroaurite and sjögrenite groups: *Amer. Mineral.* **26,** 295–306.

Gastuche, M. C., Brown, G., and Mortland, M. M. (1967) Mixed magnesium-aluminum hydroxides: *Clay Miner.* **7,** 177–201.

Giannellis, E. P., Nocera, D. G., and Pinnavaia, T. J. (1987) Anionic photocatalysts supported in layered double hydroxides: Intercalation and photophysical properties of a ruthenium complex anion in synthetic hydrotalcite: *Inorg. Chem.* **26,** 203–205.

Ingram, L. and Taylor, H. F. W. (1967) The crystal structures of sjögrenite and pyroaurite: *Mineral. Mag.* **36,** 465–479.

Mascolo, G. and Marino, O. (1980) A new synthesis and characterization of magnesium-aluminum hydroxides: *Mineral. Mag.* **43,** 619–621.

Miyata, S. (1980) Physico-chemical properties of synthetic hydrotalcites in relation to composition: *Clays & Clay Minerals* **28,** 50–56.

Miyata, S. (1983) Anion-exchange properties of hydrotalcite-like compounds: *Clays & Clay Minerals* **31,** 305–311.

Pausch, I., Lohse, H. H., Schürmann, K., and Allman, R. (1986) Synthesis of disordered and Al-rich hydrotalcite-like compounds: *Clays & Clay Minerals* **34,** 507–510.

Taylor, H. F. W. (1969) Segregation and cation-ordering in sjögrenite and pyroaurite: *Miner. Mag.* **37,** 338–342.

Taylor, R. M. (1984) The rapid formation of crystalline double hydroxy salts and other compounds by controlled hydrolysis: *Clay Miner.* **19,** 591–603.

(Received 4 September 1991; accepted 16 December 1991; Ms. 2140)

https://doi.org/10.1346/CCMN.1992.0400202 Published online by Cambridge University Press